Phytochemistry 95 (2013) 242–251

Contents lists available at ScienceDirect

Phytochemistry

journal homepage: www.elsevier.com/locate/phytochem

Anti-inflammatory phenanthrene derivatives from stems of *Dendrobium denneanum*

Yuan Lin [a,b,c], Fei Wang [a], Li-juan Yang [a], Ze Chun [a], Jin-ku Bao [b], Guo-lin Zhang [a,*]

[a] Chengdu Institute of Biology, Chinese Academy of Sciences, Chengdu 610041, PR China
[b] Key Laboratory of Bio-resources and Eco-environment (Ministry of Education), College of Life Sciences, Sichuan University, Chengdu 610064, PR China
[c] University of Chinese Academy of Sciences, Beijing 100049, PR China

ARTICLE INFO

Article history:
Received 13 May 2013
Received in revised form 3 August 2013
Available online 13 September 2013

Keywords:
Dendrobium denneanum
Orchidaceae phenanthrene
Anti-inflammatory activity
iNOS
NF-κB
MAPKs
Cytotoxic
RAW264.7 cell

ABSTRACT

Cultivated *Dendrobium denneanum* has been substituted for other endangered *Dendrobium* species in recent years, but there have been few studies regarding either its chemical constituents or pharmacological effects. In this study, three phenanthrene glycosides, three 9,10-dihydrophenanthrenes, two 9,10-dihydrophenanthrenes glycosides, and four known phenanthrene derivatives, were isolated from the stems of *D. denneanum*. Their structures were elucidated on the basis of MS and NMR spectroscopic data. Ten compounds were found to inhibit nitric oxide (NO) production in lipopolysaccharide (LPS)-activated mouse macrophage RAW264.7 cells with IC_{50} values of 0.7–41.5 μM, and exhibited no cytotoxicity in RAW264.7, HeLa, or HepG2 cells. Additionally, it was found that 2,5-dihydroxy-4-methoxy-phenanthrene 2-O-β-D-glucopyranoside, and 5-methoxy-2,4,7,9S-tetrahydroxy-9,10-dihydrophenanthrene suppressed LPS-induced expression of inducible NO synthase (iNOS) inhibited phosphorylation of p38, JNK as well as mitogen-activated protein kinase (MAPK), and inhibitory kappa B-α (IκBα). This indicated that both compounds exert anti-inflammatory effects by inhibiting MAPKs and nuclear factor κB (NF-κB) pathways.

1. Introduction

The genus *Dendrobium* Sw. (Orchidaceae) contains more than 1000 species that are wildly distributed in tropical and subtropical regions in Asia and the Pacific islands. South of the Tsinling Mountains of China, 74 species and two varieties of *Dendrobium* can be found (Zhang et al., 2003). Wild *Dendrobium* plants are nearly extinct due to increasing clinical uses in China, and have been listed as an endangered species in China and The United Nations. Stems of *Dendrobium nobile* Lindl., *Dendrobium chrysotoxum* Lindl., *Dendrobium fimbriatum* Hook. var. *oculatum* Hook., and its additional congeneric species, are recorded in the Chinese Pharmacopoeia (2010) as "Shi-Hu". These are widely used in traditional Chinese medicine for recovery of gastric motility and promoting gastric acid secretion in the stomach, as well as promoting secretion of saliva, improving eyesight, and reducing fever (Shu et al., 2004). The plants of this genus contain bibenzyls (Li et al., 2009), phenanthrenes (Lee et al., 2009; Wang et al., 2009), anthraquinones (Lin et al., 2001), fluoro-derivatives (Zhang et al., 2007), coumarins (Zhang et al., 2005), sesquiterpenes (Zhang et al., 2008) and alkaloids (Wang and Zhao, 1985). Some of these compounds have also been reported as having antioxidant, anti-inflammatory (Zhang et al., 2007), antifibrotic (Yang et al., 2007a), immunomodulatory (Zhao et al., 2001) and anti-platelet aggregation activities (Fan et al., 2001).

Dendrobium denneanum, wildly distributed in the Sichuan Province of China, is the major source of "Shi-Hu". Twelve compounds, including bibenzyls, phenanthrenes, benzoquinones, coumarins, cinnamic acid derivatives, β-sitosterol, and daucosterol, were previously isolated from the stems of *D. denneanum* (Yang et al., 2006b, 2007b; Liu et al., 2009). Due to the successful cultivation of *D. denneanum* in recent years, this plant has been a substitute for the other endangered *Dendrobium* species in clinical use. However, the compounds responsible for its pharmacological effects are still unknown.

Nitric oxide (NO) is an inflammatory mediator that plays an important role in a variety of inflammatory diseases such as arthritis, asthma, multiple sclerosis, colitis, inflammatory bowel diseases, and atherosclerosis (Guzik et al., 2003). NO is synthesized from L-arginine in a reaction catalyzed by a family of nitric oxide synthase (NOS) enzymes. Unlike other constitutively expressed NOS, inducible NOS (iNOS) is transcriptionally induced in response to bacterial endotoxins such as lipopolysaccharide (LPS), and pro-inflammatory cytokines in macrophages and various other cell types (Korhonen et al., 2005). Transcription of iNOS in

* Corresponding author. Tel./fax: +86 28 8522 9742.
E-mail address: zhanggl@cib.ac.cn (G.-l. Zhang).

0031-9422/$ - see front matter © 2013 Elsevier Ltd. All rights reserved.
http://dx.doi.org/10.1016/j.phytochem.2013.08.008

macrophages is mediated by different signaling pathways, including nuclear factor κB (NF-κB) and mitogen-activated protein kinase (MAPKs) (Thirunavukkarasu et al., 2006; Chen et al., 1998).

In this study, phytochemical experiments were carried out with the 95% ethanol extract of dried *D. denneanum* stems. Twelve phenanthrene derivatives were isolated and their structures characterized using NMR but MS spectroscopic data. Six of the isolated compounds inhibited nitric oxide (NO) production in lipopolysaccharide (LPS)-activated mouse macrophage RAW264.7 cells with IC_{50} values of 0.7–41.5 μM, but exhibited no cytotoxicity on RAW264.7, HeLa and HepG2 cells. Two compounds exert an anti-inflammatory effect by inhibiting MAPKs and NF-κB pathways.

2. Results and discussion

The air-dried stems of *Dendrobium denneanum* were extracted with 95% ethanol, and the dried extract was partitioned with petroleum ether, ethyl acetate and *n*-butanol, respectively. The ethyl acetate fraction then was subjected to repeated silica gel column chromatography and HPLC to yield compounds **1**–**12**. The structures of these compounds are shown in Fig. 1.

Compound **1** was obtained as a colorless colloidal solid. Its molecular formula was determined to be $C_{21}H_{22}O_8$ from the quasi molecular ion peak at 425.1208 in the HR-ESI-MS ($[M+Na]^+$). Its UV maxima absorptions at 214.5, 254.0, 283.5, and 313.5 nm were similar to phenanthrene derivatives (Ito et al., 2010). Its ^1H NMR (Table 1) signals at 7.44 (t, J = 7.6 Hz, H-7), 7.40 (d, J = 7.6 Hz, H-8), 7.13 (dd, J = 7.6, 1.4 Hz, H-6) showed a 1,2,3-trisubstituted phenyl ring. The ^1H NMR resonances at δ 7.54 and 7.62 (each d, J = 8.8 Hz) could be respectively assigned to H-9 and H-10 of the phenanthrene. The other two aromatic protons were observed at δ 7.33 and 7.20 (each d, J = 2.0 Hz, H-1 and H-3). A methoxy group was determined based on the ^1H NMR signals at δ 4.10 and the ^{13}C NMR resonance at δ 59.1 (Table 1). The NOESY correlation between H-1 and H-10, and between $-OCH_3$ and H-3, suggested that the methoxy group is at C-4. Acid hydrolysis of **1** afforded D-glucose, which was determined by GC–MS and by the molecular rotation ($[M]_D$ −209.0) of **1** and methyl-β-D-glucopyranoside ($[M]_D$ −66.3) (Devkota et al., 2012; Khurelbat et al., 2010) according to Klyne's rule (Klyne, 1950). The D-glucopyranosyloxyl moiety supported by the ^1H NMR signal at δ 5.11 (d, J = 7.3 Hz, H-1′) and the ^{13}C NMR resonances at δ 102.7, 78.6, 78.2, 75.2, 71.8 and 62.8 could be located at C-2 from the HMBC correlations of H-1′ with C-2 (δ 157.9) (Fig. 2). From the IR absorption at 3427 cm^{-1} and the molecular formula, a hydroxyl group was postulated, which could be located at C-5 in view of the HMBC correlations of H-9 with C-8, and H-8 with C-9. Structure **1** was thus elucidated as 2,5-dihydroxy-4-methoxy-phenanthrene 2-O-β-D-glucopyranoside.

Compound **2**, obtained as a yellowish colloidal solid, has the molecular formula $C_{26}H_{30}O_{12}$ as determined by the quasi molecular ion peak at 557.1629 in the HR-ESI-MS ($[M+Na]^+$). The presence of hydroxyl groups was suggested by the IR absorption at 3434 cm^{-1}. Its UV maxima absorptions at 214.5, 254.0, 283.5 and 313.5 nm also indicated a phenanthrene derivative (Ito et al., 2010). Its NMR spectroscopic data (Table 1) of compound **2** were very similar to those of compound **1**, except that **2** contained one more sugar residue. A β-apiofuranosyl was provided by the ^1H NMR signal at δ 5.00 and the ^{13}C NMR signals at δ 111.1, 78.2, 80.6, 75.1 and 65.7. The absolute configuration of the D-apiofuranosyl moiety in **2** was confirmed by the molecular rotation difference ($[M]_D$ of **2** − $[M]_D$ of **1** = −501.2) (Takayanagi et al., 2003). The HMBC correlations of H-1with C-6 (δ 68.9) indicated that compound **2** contains a β-D-apiofuranosyl-(1–6)-β-D-glucopyranosyl moiety (Fig. 2). Thus, compound **2** was determined to be 2,5-dihydroxy-4-methoxy-phenanthrene 2-O-β-D-apiofuranosyl-(1–6)-β-D-glucopyranoside.

Compound **3**, was obtained as a yellowish colloidal solid, and molecular formula was determined to be $C_{27}H_{32}O_{12}$, through the quasi molecular ion peak at 571.1794 in the HR-ESI-MS ($[M+Na]^+$). Its IR absorption at 3441 cm^{-1} showed the presence of hydroxyl groups. Its UV maxima absorptions at 214.5, 254.0, 283.5 and 313.5 nm again indicated a phenanthrene derivative (Ito et al., 2010). The NMR spectroscopic data confirmed that compound **3** possessed the same skeleton and substitution mode as compound **1**, except that it contained an extra sugar residue. The α-rhamnopyranosyl group was deduced from the ^1H NMR signal at δ 4.71 and the ^{13}C NMR signals at δ 102.3, 72.3, 72.7, 74.3, 70.1 and 18.1, respectively. Its absolute configuration of L-rhamnopyranosyl moiety in **2** was confirmed by the molecular rotation difference ($[M]_D$ of **3** − $[M]_D$ of **1** = −580.1) (Okamura et al., 1981). The HMBC correlation between H-1″ (δ 4.71) with C-6′ (δ 68.0) indicated that compound **3** contains an α-L-rhamnopyranosyl-(1–6)-β-D-glucopyranosyl moiety (Fig. 2). Thus, compound **3** was

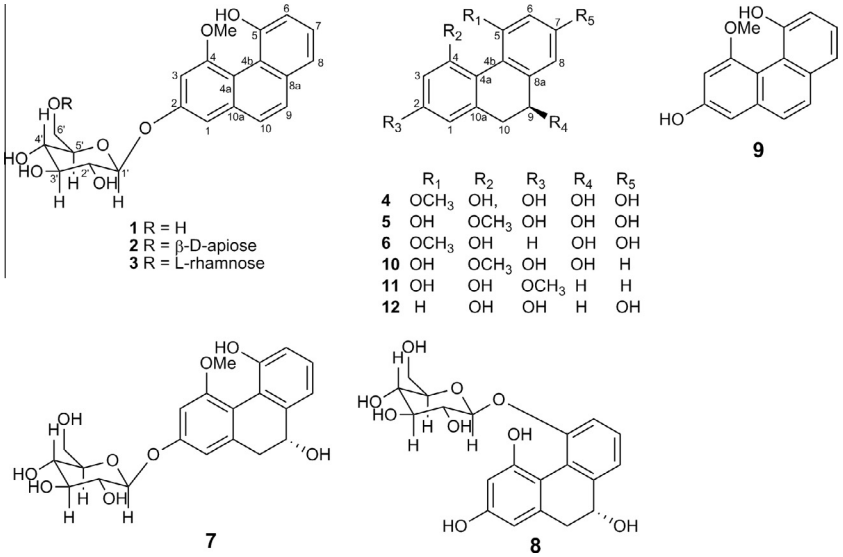

	R_1	R_2	R_3	R_4	R_5
4	OCH_3	OH,	OH	OH	OH
5	OH	OCH_3	OH	OH	OH
6	OCH_3	OH	H	OH	OH
10	OH	OCH_3	OH	OH	H
11	OH	OH	OCH_3	H	H
12	H	OH	OH	H	OH

Fig. 1. Compounds **1**–**12** isolated from *Dendrobium denneanum*.

Table 1
^{1}H and ^{13}C NMR (600 and 150 MHz, MeOH-d_4) spectroscopic data of compounds **1–3** (δ in ppm, multiplicities, J in Hz).

Position	**1**		**2**		**3**	
	δ_C	δ_H	δ_C	δ_H	δ_C	δ_H
1	109.7	7.33 d (2.0)	109.7	7.32 d (2.4)	109.6	7.31 d (2.4)
2	157.9	–	157.8	–	157.8	–
3	104.0	7.20 d (2.0)	104.2	7.17 d (2.4)	104.3	7.17 d (2.4)
4	156.7	–	156.7	–	156.8	–
4a	116.5	–	116.5	–	116.6	–
4b	119.9	–	119.9	–	119.9	–
5	155.4	–	155.4	–	155.4	–
6	117.4	7.13 dd (7.6, 1.4)	117.4	7.13 dd (7.6, 1.4)	117.4	7.12 dd (7.6, 1.4)
7	128.3	7.44 t (7.6)	128.3	7.45 t (7.6)	128.3	7.45 t (7.6)
8	121.8	7.40 d (7.6)	121.7	7.40 d (7.6)	121.8	7.41 dd (7.6, 1.1)
8a	136.0	–	136.0	–	136.0	–
9	130.3	7.62 d (8.8)	130.3	7.64 d (8.8)	130.5	7.67 d (8.8)
10	127.7	7.54 d (8.8)	127.8	7.56 d (8.8)	127.8	7.56 d (8.8)
10a	137.4	–	137.4	–	137.4	–
4-OCH_3	59.1	4.10 s	59.2	4.10 s	59.3	4.10 s
1′	102.7	5.11 d (7.3)	102.6	5.09 d (7.2)	102.5	5.10 d (7.2)
2′	75.2	3.57 m	75.1	3.54 m	75.1	3.54 m
3′	78.2	3.57 m	78.1	3.54 m	78.2	3.54 m
4′	71.8	3.42 m	71.8	3.20 m	71.7	3.41 m
5′	78.6	3.57 m	77.3	3.72 m	77.2	3.69 m
6′	62.8	3.97 dd (12.1, 2.2) 3.73 dd (12.1, 6.3)	68.9	4.10 m 3.65 dd (11.0, 6.7)	68.0	4.10 m 3.62 dd (11.0, 6.5)
1″	–	–	111.1	5.00 d (2.4)	102.3	4.71 d (1.2)
2″	–	–	78.2	3.94 d (2.4)	72.3	3.85 m
3″	–	–	80.6		72.7	3.73 dd (9.5, 3.4)
4″	–	–	75.1	4.00 d (9.6) 3.75 d (9.6)	74.3	3.35 m
5″	–	–	65.7	3.58 s	70.1	3.66 dd (9.5, 6.1)
6″	–	–	–	–	18.1	1.17 d (6.2)

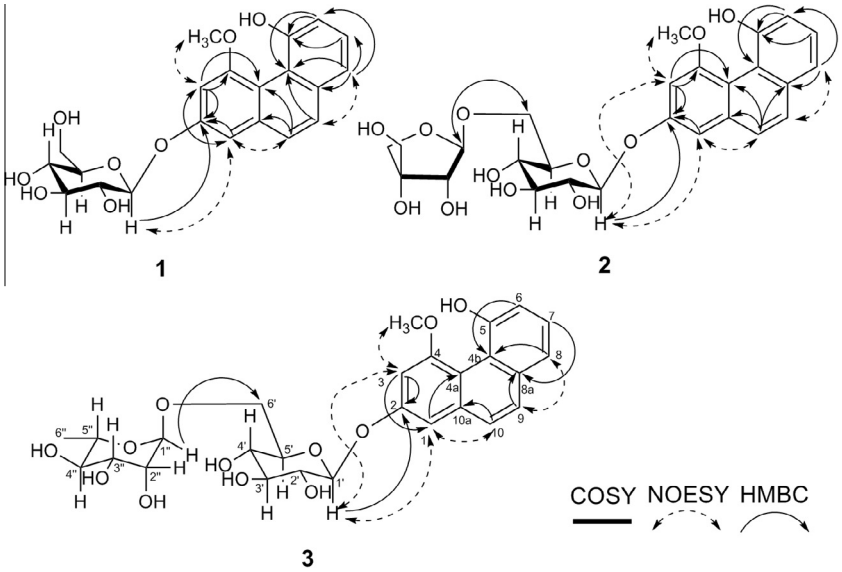

Fig. 2. Key ^{1}H–^{1}H COSY, HMBC and NOESY correlations of compounds **1**–**3**.

2,5-dihydroxy-4-methoxy-phenanthrene 2-O-α-L-rhamnopyranosyl-(1–6)-β-D-glucopyranoside.

Compound **4** was obtained as a yellowish powder. Its molecular formula was determined to be $C_{15}H_{14}O_5$ from the quasi molecular ion peak at 297.0736 in the HR-ESI-MS ([M+Na]$^+$). Its UV maxima absorptions at 211.0, 274.5 and 307.0 nm were similar to those of 9,10-dihydrophenanthrene derivatives (Yoshikawa et al., 2012). Its ^{1}H NMR spectrum (Table 2) exhibited signals for two pairs of meta-coupled aromatic protons at δ 6.35 (d, J = 2.5 Hz, H-1), 6.30 (d, J = 2.5 Hz, H-3), 6.56 (d, J = 2.4 Hz, H-6) and 6.82 (d, J = 2.4 Hz, H-8), two methylene protons at δ 2.76 (dd, J = 13.8, 3.9 Hz, H-10), 2.68 (dd, J = 13.8, 11.0 Hz, H-10), and one methine proton at δ 4.47 (dd, J = 11.0, 3.9 Hz). A methoxy group was presumed from the ^{1}H NMR resonances at δ 3.90 and the ^{13}C NMR signal at δ 58.0 (Table 2). The NOESY correlations between H-10 and H-1, H-8 and H-9, OCH_3 and H-6 confirmed the location of the 5-OCH_3 group (Fig. 3). Based on the IR absorption at 3420 cm^{-1}, its molecular formula and oxygenated C-atoms (δ 158.4, 154.2, 158.8, 70.1), four hydroxyl groups were assumed. The HMBC correlations (H-1/C-2, C-3, C-4a; H-3/C-4, C-4a; H-6/C-4b, C-5, C-7; H-8/C-4b, C-6, C-7; H-10/C-4a, C-8a, C-10a) suggested that the four hydroxyl groups were located at C-2, C-4, C-7 and C-9. The CD spectra

Table 2
^{1}H and ^{13}C NMR (600 and 150 MHz, MeOH-d_4) spectroscopic data of compounds **4**–**6** (δ in ppm, multiplicities, J in Hz).

Position	**4**		**5**		**6**	
	δ_C	δ_H	δ_C	δ_H	δ_C	δ_H
1	109.8	6.35 d (2.5)	111.7	6.50 d (2.3)	121.8	6.83 m
2	158.4	–	158.7	–	128.8	7.08 t (7.7)
3	105.2	6.30 d (2.5)	101.3	6.53 d (2.3)	118.8	6.83 m
4	154.2	–	156.1	–	154.5	–
4a	113.6	–	113.6	–	121.7	–
4b	114.3	–	112.7	–	113.7	–
5	156.0	–	155.8	–	156.8	–
6	101.4	6.56 d (2.4)	105.5	6.34 d (2.6)	101.1	6.59 d (2.3)
7	158.8	–	158.7	–	160.0	–
8	107.6	6.82 d (2.4)	106.1	6.64 brs	108.4	6.83 d (2.3)
8a	145.9	–	143.3	–	147.8	–
9	70.1	4.47 dd (11.0, 3.9)	70.2	4.47 dd (11.0, 3.9)	70.1	4.49 dd (11.0, 3.9)
10	41.3	2.76 dd (13.8, 3.9) 2.68 dd (13.8, 11.0)	41.0	2.76 dd (13.8, 3.9) 2.68 dd (13.8, 11.0)	57.9	2.85 dd (13.8, 3.9) 2.68 dd (13.8, 11.0)
10a	139.0	–	139.6	–	137.9	–
4-OCH_3	–	–	57.9	3.91 s	–	–
5-OCH_3	58.0	3.90 s	–	–	57.9	3.93 s

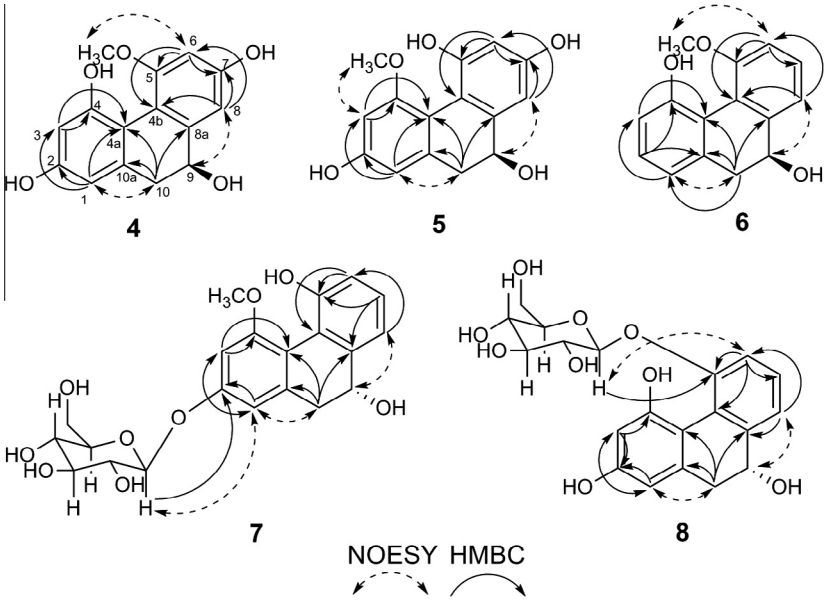

Fig. 3. Key HMBC and NOESY correlations of compounds **4**–**8**.

of both **4** and (9S)-hydroxy-9,10-dihydrophenanthrene (Resnick and Gibson, 1996) showed a negative Cotton effect at 234 nm and a positive Cotton effect at 268 nm, indicating a 9S configuration of **4**. Therefore, compound **4** was 5-methoxy-2,4,7,9S-tetrahydroxy-9,10-dihydrophenanthrene.

Compound **5**, obtained as a yellowish powder, has the molecular formula $C_{15}H_{14}O_5$, as established by the quasi molecular ion peak at 297.0736 in the HR-ESI-MS ($[M+Na]^+$). Its IR spectrum showed the presence of hydroxyl groups (3439 cm^{-1}). Its UV maxima absorptions at 211.5, 274.5 and 306.0 nm are similar to 9,10-dihydrophenanthrene derivatives (Yoshikawa et al., 2012). The mass and NMR spectroscopic data were similar to those of compound **4**. The NMR (Table 2), NOESY and HMBC spectra (Fig. 3) supported the structure of **5**. The CD spectra of **5** and (+)-(9S)-hydroxy-9,10-dihydrophenanthrene (Resnick and Gibson, 1996) are similar, with a negative Cotton effect at 234 nm and a positive Cotton effect at 268 nm. Thus, compound **5** was elucidated to be 4-methoxy-2,5,7,9S-tetrahydroxy-9,10-dihydrophenanthrene.

Compound **6** was obtained as a yellowish powder. Its molecular formula was established to be $C_{15}H_{14}O_4$ from the quasi molecular ion peak at 281.0784 in the HR-ESI-MS ($[M+Na]^+$). Its maxima IR absorption at 3434 cm^{-1} indicated the presence of hydroxyl groups, whereas UV maxima absorptions at 212.0, 272.5 and 303.0 nm were similar to other 9,10-dihydrophenanthrene derivatives (Yoshikawa et al., 2012). Its NMR (Table 2), NOESY and HMBC spectra (Fig. 3) supported the structure of **6**. The CD spectra of **6** and (+)-(9S)-hydroxy-9,10-dihydrophenanthrene (Resnick and Gibson, 1996) showed a negative Cotton effect at 234 nm and a positive Cotton effect at 268 nm. Therefore, structure **6** was 5-methoxy-4,7,9S-trihydroxy-9,10-dihydrophenanthrene.

Compound **7** was obtained as a yellowish colloidal solid. Its molecular formula was determined to be $C_{21}H_{24}O_9$ from the quasi molecular ion peak at 443.1318 in the HR-ESI-MS ($[M+Na]^+$). The IR spectrum indicated hydroxyl groups (3398 cm^{-1}). The UV maxima absorptions at 211.0, 270.0 and 302.0 nm were similar to 9,10-dihydrophenanthrene derivatives (Yoshikawa et al., 2012). Two methylene protons at 2.85 (dd, J = 14.3, 3.4 Hz, H-10), 2.79 (dd, J = 14.3, 9.6 Hz, H-10), one methoxy proton at 3.96 (s), and one methine proton at 4.57 (brs) were deduced from the ^{1}H NMR spectrum. Its NOESY and HMBC correlations (Fig. 3) supported the

Table 3
^{1}H and ^{13}C NMR (600 and 150 MHz, MeOH-d_4) spectroscopic data of compounds **7, 8** (δ in ppm, multiplicities, J in Hz).

Position	**7**		**8**	
	δ_C	δ_H	δ_C	δ_H
1	112.5	6.79 brs	109.9	6.38 d (2.2)
2	159.3	–	159.3	–
3	102.2	6.87 brs	105.4	6.34 d (2.4)
4	156.5	–	156.4	–
4a	117.4	–	113.4	–
4b	120.5	–	123.2	–
5	154.8	–	152.8	–
6	119.6	6,91 dd (7.7, 1.2)	116.3	7.29 m
7	129.4	7,21 t (7.7)	128.6	7.29 m
8	118.3	7.11 d (7.7)	120.2	7.29 m
8a	143.8	–	143.5	–
9	69.8	4.57 brs	69.9	4.57 dd (10.2, 4.0)
10	40.7	2.85 dd (14.3, 3.4) 2.79 dd (14.3,9.6)	41.2	2.78 dd (13.8, 4.0) 2.71 dd (13.8, 10.2)
10a	140.2	–	139.7	–
4-OCH_3	57.8	3.96 s	–	–
Glc-1	102.5	5.07 d (7.2)	102.1	5.10 d (7.6)
Glc-2	75.1	3.49 m	74.9	3.47 m
Glc-3	78.1	3.45 m	78.2	3.47 m
Glc-4	71.8	3.37 m	71.3	3.40 m
Glc-5	78.5	3.45 m	78.5	3.47 m
Glc-6	62.9	3.93 dd (12.1, 2.0) 3.68 dd (12.1, 6.5)	62.7	3.87 d (11.4) 3.68 dd (12.2, 5.5)

Table 4
Effects of phenanthrene derivatives (**1–12**) on cell viability in RAW 264.7 cells, HeLa cells and HepG2 cells.

Compounds	RAW 264.7(%)			HeLa(%)	HepG2(%)
	100 μM	50 μM	1 μM	50 μM	50 μM
1	61 ± 2	124 ± 9	101 ± 3	98 ± 3	72 ± 3
2	58 ± 1	93 ± 2	93 ± 3	95 ± 3	87 ± 4
3	92 ± 3	90 ± 2	89 ± 9	96 ± 5	99 ± 2
4	51 ± 2	105 ± 8	97 ± 2	105 ± 7	100 ± 5
5	53 ± 5	93 ± 4	95 ± 3	94 ± 8	95 ± 2
6	67 ± 2	124 ± 15	97 ± 3	96 ± 8	92 ± 2
7	55 ± 6	93 ± 9	106 ± 14	89 ± 8	100 ± 5
8	56 ± 4	102 ± 6	105 ± 4	95 ± 2	109 ± 1
9	47 ± 3	86 ± 2	79 ± 8	106 ± 11	89 ± 3
10	54 ± 1	82 ± 7	80 ± 9	96 ± 4	109 ± 5
11	64 ± 2	83 ± 1	97 ± 3	95 ± 3	92 ± 3
12	88 ± 8	96 ± 2	94 ± 6	96 ± 1	93 ± 3

The values are mean ± SEM (n = 3).

assignment of the 4-OCH_3, 5-OH and 9-OH. Acid hydrolysis of **7** afforded D-glucose, which was determined by GC–MS and by its optical rotation {[α] $^{25}_D$ +51.1 (c 0.3, H_2O)}. The β-D-glucopyranosyloxyl moiety was presumed based on the ^{1}H NMR signal at δ 5.07 (d, J = 7.2 Hz, H-1) and ^{13}C NMR resonances at δ 102.5, 78.5, 78.1, 75.1, 71.8 and 62.9, which could be located at C-2 from the HMBC correlation of H-1′ and C-2. The CD spectrum of **7** (negative/positive Cotton effects: 234 nm/268 nm) is opposite to that of (+)-(9S)-hydroxy-9,10-dihydrophenanthrene (Resnick and Gibson, 1996). Thus, structure **7** was 4-methoxy-2,5,9R-trihydroxy-9,10-dihydrophenanthrene 2-O-β-D-glucopyranoside.

Compound **8**, obtained as a colorless colloidal solid, has the molecular formula $C_{20}H_{22}O_9$, as established by the molecular ion peak at 428.1156 in the HR-ESI-MS ([M+Na]$^+$). Its IR spectrum showed the presence of hydroxyl groups (3420 cm^{-1}). Its UV maxima absorptions at 211.0, 275.0 and 302.0 nm, were similar to 9,10-dihydrophenanthrene derivatives (Yoshikawa et al., 2012). The ^{1}H NMR and ^{13}C NMR spectroscopic data (Table 3) were similar to those of compound **7**, but with no methoxyl group detected.

Table 5
Effects of compounds **1–12** on LPS-Induced NO production in RAW264.7 cells.

Compounds	% Inhibition on LPS-induced NO production			IC_{50} (μM)
	50	10	1	
1	92 ± 2	78 ± 4	38 ± 3	4.6
2	76 ± 4	44 ± 7	24 ± 5	16.9
3	62 ± 1	30 ± 3	24 ± 1	41.5
4	90 ± 7	80 ± 2	27 ± 8	3.1
5	86 ± 2	78 ± 3	42 ± 4	4.2
6	58 ± 8	50 ± 9	44 ± 5	–
7	68 ± 2	60 ± 1	40 ± 8	–
8	92 ± 5	77 ± 2	62 ± 2	0.7
9	95 ± 6	75 ± 4	30 ± 1	6.3
10	82 ± 5	39 ± 1	21 ± 3	27.4
11	95 ± 3	69 ± 2	38 ± 4	7.6
12	74 ± 6	43 ± 3	27 ± 5	32.7
Curcumin[a]	84 ± 3	72 ± 2	30 ± 4	6.2

The values are mean ± SEM (n = 3).
[a] Curcumin was used as a positive control.

Acid hydrolysis of **8** afforded D-glucose, which was determined by GC–MS and by its optical rotation {[α] $^{25}_D$ +51.4 (c 0.4, H_2O)}. The β-D-glucopyranosyloxyl provided by the ^{1}H NMR signal at δ 5.10 (d, J = 7.6 Hz, H-1¢) and the ^{13}C NMR signals at δ 102.1, 78.5, 78.2, 74.9, 71.3 and 62.7 and which could be located at C-2 from the HMBC correlations of H-1¢ with C-5. Based on the molecular formula $C_{20}H_{22}O_9$, three hydroxyl groups could be presumed, and are likely located at C-2, C-4 and C-9 on the basis of the NOESY and HMBC experiments. The CD spectrum of **8** (negative/positive Cotton effects: 234 nm/268 nm) is opposite to that, (+)-(9S)-hydroxy-9,10-dihydrophenanthrene (Resnick and Gibson, 1996). Thus, structure **8** was 1,2,5,9R-tetrahydroxy-9,10-dihydrophenanthrene 5-O-β-D-glucopyranoside.

Compounds **1** and **9** might be aromatized from compounds **7** and **10** during the silica gel column chromatography. Thus, a test was carried out to study the impact of silica gel and solvent on the stability of compounds **1** and **9**. Thus, a mixture of compound **7** (or **10**, 0.5 mg), silica gel (25.0 mg) and methanol (0.3 mL) in a test tube was heated at 45 °C for 24 h. Each suspension was filtered and the filtrate so obtained was analyzed by HPLC (Fig. S44 and S45). These results indicated that dehydration had not occurr in presence of silica gel in our test and provided preliminary evidence toward the natural occurrence of compounds **1** and **9**.

Cytotoxic effects of compounds **1–12** were examined in mouse macrophage RAW264.7 cells, human cervical cancer HeLa cells and human hepatoma HepG2 cells. As shown in Table 4, compounds **1–12** had no cytotoxic activity in these cells at 50 μM. Compounds **1**, **2**, and **4–11** showed weak cytotoxic activity in RAW264.7 macrophages at 100 μM.

Phenanthrenes, the major components of *D. denneanum*, were also obtained from species of the Orchidaceae family, including *Bulbophyllum*, *Eria*, *Maxillaria*, *Bletilla*, *Coelogyna*, *Cymbidium*, *Ephemerantha* and *Epidendrum* (Adriána et al., 2008). Phenanthrenes have been found to have various biological activities such as anti-inflammatory (Yang et al., 2006a), cytotoxic (Lee et al., 2009), antifibrotic (Yang et al., 2007a), anticancer (Lee et al., 1995), and antimicrobial (Adriána et al., 2008) effects. To determine if the isolated compounds were responsible for the anti-inflammatory effects of this plant in clinical use, compounds **1–12** (Fig. 1) were tested for their effects on LPS-induced NO production in RAW264.7 cells. As shown in Table 5, compounds **1**, **4**, **5**, **8**, **9** and **11** potently inhibited NO production with IC_{50} values of 0.7–7.6 μM, whereas compounds **2**, **3**, **10**, and **12** showed only moderate inhibitory activity with IC_{50} values of 16.9–41.5 μM. The inhibitory effects of compounds **9** and **10** on NO production (IC_{50} = 6.3, 27.4 μM) were similar as those reported (IC_{50} = 6.4, 29.1 μM) (Ito

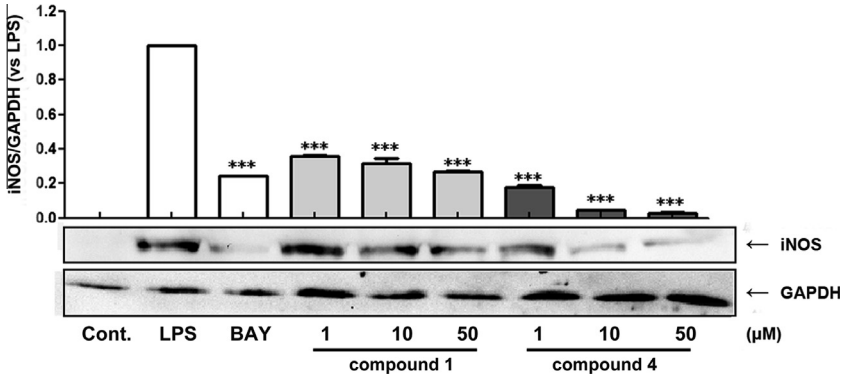

Fig. 4. Effect of compounds **1** and **4** on the expression of iNOS. RAW264.7 cells were pretreated with compounds **1** and **4** (1, 10, 50 μM) and a positive control (BAY) for 2 h, and then treated with LPS for 18 h. Cell lysates were immunoblotted with an anti-iNOS antibody. GAPDH staining is shown as a loading control. The quantitative results are depicted. Cont. (control), DMSO; LPS, 1 μg/mL lipopolysaccharide; BAY, 10 μM BAY 11-7082. $^{***}p < 0.001$ compared with the LPS group.

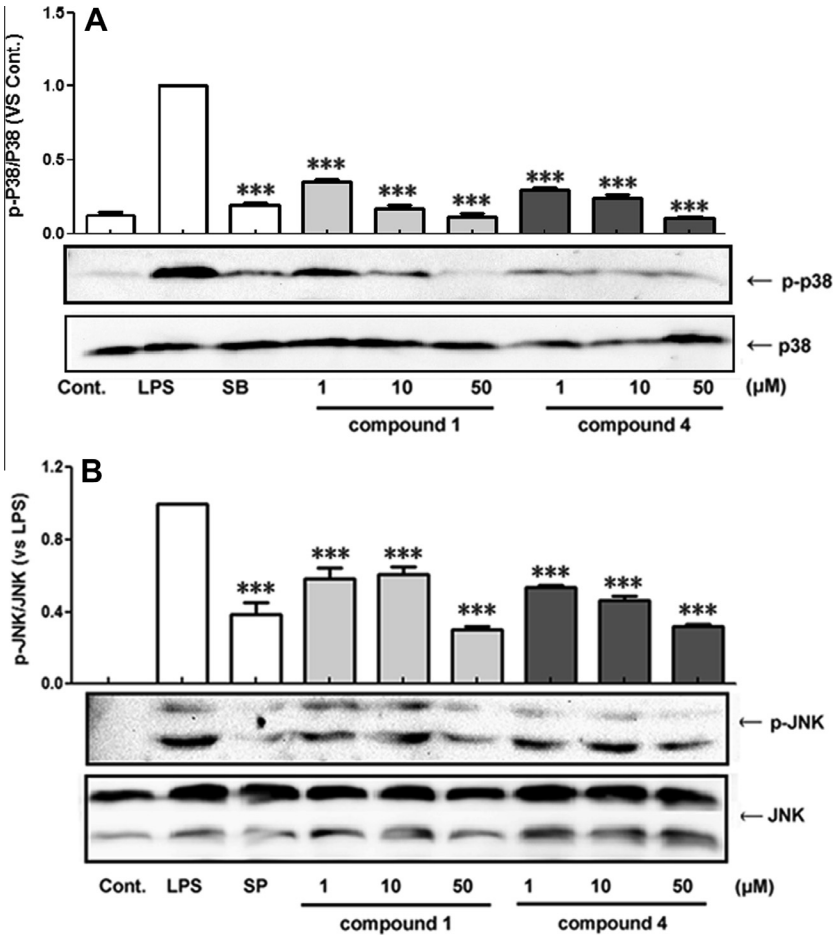

Fig. 5. Effect of compounds **1** and **4** on the phosphorylation of p38 and JNK. (A) RAW264.7 cells were pretreated with compounds **1** and **4** (1, 10, 50 μM) and a positive control for 2 h and treated with LPS for 30 min. Cell lysates were immunoblotted with an anti-phospho-p38 antibody (Thr180/Tyr182). The total p38 staining was used as an internal control. The quantitative results are depicted. Cont., DMSO; LPS, 1 μg/mL lipopolysaccharide; SB, 10 μM SB203580. (B) RAW264.7 cells were pretreated with compounds **1** and **4** (1, 10, 50 μM) and a positive control for 2 h and treated with LPS for 30 min. Cell lysates were immunoblotted with an anti-phospho-JNK antibody (Thr183/Tyr185). The total JNK staining was used as an internal control. The quantitative results are depicted. Cont., DMSO; LPS, 1 μg/mL lipopolysaccharide; SP, 20 μM SP600125. $^{***}p < 0.001$ compared with the LPS group.

et al., 2010) in LPS-activated RAW264.7 cells, thus indicating that our assay is suitable for the evaluation of NO production.

NO is a well-known pro-inflammatory cytokine involved in many inflammatory diseases (Guzik et al., 2003). Compounds **1–12** may act as the anti-inflammatory chemical compounds in *D. denneanum*, and therefore, may be suitable substitutes for other endangered species for the prevention and treatment of inflammatory diseases in a clinical setting (Chinese Pharmacopoeia, 2010). The anti-inflammatory activities of these phenanthrenes (**1–3, 9**) suggest that attached disaccharide moieties could reduce their activity: compounds **2** and **3,** with a disaccharide, were much less active (IC_{50} = 16.9, 41.5 μM) than compounds **1** and **9,** with or

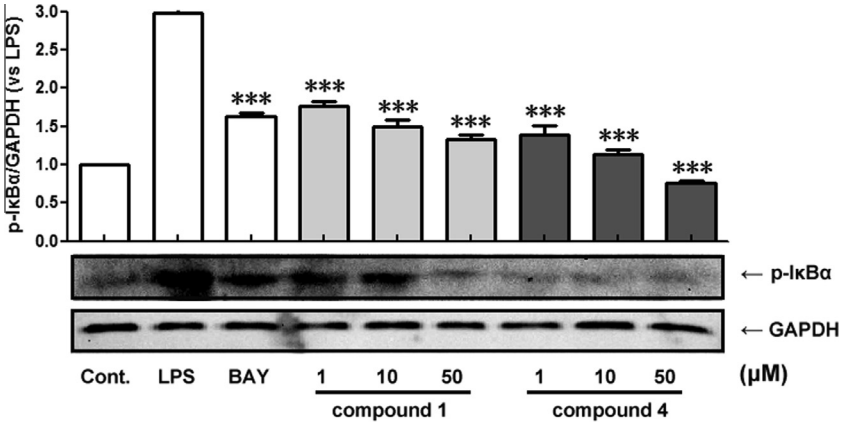

Fig. 6. Effect of compounds **1** and **4** on the phosphorylation of IκBα. RAW264.7 cells were pretreated with compounds **1** and **4** (1, 10, 50 μM) and a positive control (BAY) for 2 h, and then treated with LPS for 20 min. Cell lysates were immunoblotted with an anti-phospho-IκBα antibody (Ser32/36). GAPDH staining is shown as a loading control. The quantitative results are depicted. Cont., DMSO; LPS, 1 μg/mL lipopolysaccharide; BAY, 10 μM BAY 11-7082. $^{***}p < 0.001$ compared with the LPS group.

without a sugar moiety (IC_{50} = 4.6, 6.3 μM). For the class of 9-hydroxy-9,10-dihydrophenanthrenes (**4–8**, **10**), a hydroxyl group at C-2 was necessary for increasing activity: the activity of compounds **4**, **5**, **8** and **10** were more potent than compounds **6** and **7**.

To further study the mechanism of these compound-mediated inhibition of NO production, the protein expression of iNOS, the major enzyme catalyzing the formation of NO, was examined. As shown in Fig. 4, LPS treatment significantly increased iNOS expression. BAY 11-7082, a NF-κB inhibitor, used as a positive control (Mendes et al., 2009), inhibited LPS-induced iNOS expression. Pretreatment with compounds **1** and **4** (1–50 μM), significantly blocked LPS-Induced iNOS expression in a concentration-dependent manner, indicating that these compounds could decrease NO production in LPS-activated RAW264.7 cells by inhibiting iNOS expression.

Phosphorylation of p38 and JNK MAPK has been shown to regulate expression of iNOS and other pro-inflammatory cytokines (Sung et al., 2009; Thirunavukkarasu et al., 2006); thus, the effects of compounds **1** and **4** on p38 and JNK MAPK phosphorylation were examined. As shown in Fig. 5A, LPS significantly increased phosphorylation of p38. SB203580, a specific p38 MAPK inhibitor (Lee et al., 1994; Badger et al., 1998), inhibited the p38 phosphorylation stimulated by LPS. Pretreatment with compounds **1** and **4** (1–50 μM) also significantly inhibited LPS-stimulated p38 MAPK phosphorylation in a concentration-dependent manner. LPS can also stimulate JNK phosphorylation in RAW264.7 cells, as previously reported. As shown in Fig. 5B, SP600125, a specific JNK MAPK inhibitor, significantly blocked LPS-activated JNK phosphorylation (Bennett et al., 2001). Pretreatment with compounds **1** and **4** (1–50 μM) also significantly inhibited LPS-stimulated JNK phosphorylation in a concentration-dependent manner. These results suggest that these compounds could decrease iNOS expression by inhibiting phosphorylation of p38 and JNK MAPK. AP-1 (activating proteins 1), sequencing specific transcription factors, have also been shown to be key regulatory molecules in the control of inflammatory responses. MAPKs, including ERK, p38, and JNK have been reported to facilitate binding of AP-1 transcription factors with promoters of pro-inflammatory cytokines (Ono and Han, 2000; Karin, 1995). Thus, it is possible that compounds **1** and **4** decrease pro-inflammatory cytokine expression via inhibition of AP-1, by inhibiting phosphorylation of p38 and JNK MAPKs.

Phosphorylation of inhibitory kappa B α (IκBα) plays a key role in regulation of NF-κB function in transcription of pro-inflammatory cytokines (Sung et al., 2009; Khan et al., 2011). Thus, the effects of compounds **1** and **4** on IκBα phosphorylation were investigated. As shown in Fig. 6, LPS significantly activated the phosphorylation of IκBα. BAY 11-7082, an IκB inhibitor, inhibited the phosphorylation of IκBα induced by LPS. Compounds **1** and **4** (1–50 μM) significantly inhibited the LPS-stimulated IκBα phosphorylation in a concentration-dependent manner. This result indicated that these compounds may decrease NF-κB-mediated pro-inflammatory cytokine production by inhibiting IκBα phosphorylation. NF-κB transcription factors play a key role in regulating the expression of numerous genes involved in inflammation. Activation of NF-κB depends on phosphorylation of IκBα and subsequent ubiquitination and degradation of IκBα proteins. After degradation of IκBα, NF-κB translocates to the nucleus and exerts its transcription function (Quivy and Lint, 2004). In this study, it was found that IκBα phosphorylation was significantly inhibited by compounds **1** and **4**, which prevents the degradation of IκBα and subsequent NF-κB activation. Therefore, compounds **1** and **4** may decrease the expression of pro-inflammatory cytokines by inhibiting the activation of NF-κB mediated by phosphorylation of IκBα. Previously 2,5-dimethoxy-1,7-dihydroxy-9,10-dihydrophenanthrene was found to inhibit the MAPK and NF-κB pathways, mimicking a TLR4 (toll-like receptor 4 antagonist) (Datla et al., 2010); hence, further study is needed to examine if compounds **1** and **4** exert their anti-inflammatory effects by inhibiting LPS-induced toll-like receptor activation.

3. Conclusion

Eight new compounds were isolated from the stems of *D. denneanum*: three new phenanthrene glycosides (**1–3**), three new 9,10-dihydrophenanthrenes (**4–6**) and two new 9,10-dihydrophenanthrenes glycosides (**7** and **8**). The new compounds (**1**, **4**, **5** and **8**) showed potent anti-inflammatory activity in LPS-induced NO production in RAW264.7 cells with IC_{50} values of 0.7–4.6 μM. Compounds **1** and **4** inhibited NO production by blocking iNOS expression, p38 MAPK phosphorylation and IκBα phosphorylation. These results indicated that the chemical composition of *D. denneanum* was similar to other species of *Dendrobium*, and validated its clinical use as a substitute for other endangered *Dendrobium* species. Compounds **1** and **4** warrant further investigation as new pharmaceutical tools for prevention and treatment of inflammatory diseases.

4. Experimental

4.1. General experimental procedures

UV Spectra were recorded on a UV1902 spectrophotometer, whereas optical rotation $[\alpha]_D$ values were determined with a Perkin–Elmer 341 automatic polarimeter, and IR spectra were measured on a Perkin–Elmer FT-IR spectrometer (KBr disc). CD spectra were obtained on a JASCO J-810 spectrometer. NMR spectra were recorded in MeOH-d_4 on a Bruker Avance 600 NMR spectrometer. MS data was obtained on a Bruker Daltonics Bio-TOF-Q mass spectrometer. Column chromatography (CC) was carried out on silica gel (200–300 mesh, Qingdao Haiyang Chemical CO., Ltd.). Silica gel GF 254 pre-coated plates (Qingdao Haiyang Chemical Inc., Qingdao, P. R. China) were used for preparative TLC. Sephadex LH-20 was purchased from Pharmacia Biotech (Sweden). HPLC analysis was performed using a 250 mm × 20 mm, 5 μm, Kromasil 100-10-C18 column on an Agilent 1260 HPLC system.

4.2. Plant material

Fresh stems of *Dendrobium denneanum* were collected in April 2010 from Jiajiang, Sichuan Province, P. R. China and identified by Prof. Ze Chun at the Chengdu Institute of Biology, Chinese Academy of Science (CAS). A voucher specimen (LD-0) is deposited in the Herbarium of Chengdu Institute of Biology, CAS.

4.3. Extraction and isolation

Air-dried stems of *Dendrobium denneanum* (15 kg) were extracted with EtO4–H_2O (3 × 70 L, 95:5, v/v, each 6 days duration) at room temperature. The filtrates were combined and concentrated under reduced pressure at 45 °C to obtain an EtO_4 (1.1 kg). The latter was suspended in H_2O (4 L) and partitioned successively with petroleum ether (6 × 4 L), $EtoA_2$ (6 × 4 L) and *n*-butanol (6 × 4 L). The $EtoA_2$ fraction (150.0 g) was divided into 7 subfractions (Fr. 1–7) over a silica gel column eluted with $CHCl_3$-MeOH (30:1, 10:1, 0:1).

Fr.3 (9.4 g) was separated by a Sephadex (LH-20) CC eluted with $CHCl_3$-MeOH (1:1) to yield Fr.3.1–Fr.3.2. Subsequently, Fr.3.2. (2.1 g) was separated by a silica gel CC and eluted with $CHCl_3$-MeOH (25:1) to give 6 subfractions (Fr.3.2.1–Fr.3.2.6). Separation of Fr.3.2.2 by HPLC (MeOH/H_2O, 1:1) afforded **6** (1.5 mg).

Fr.6 (40.7 g) was separated using a Sephadex (LH-20) CC and eluted with $CHCl_3$-MeOH (1:1) to yield Fr.6.1–Fr.6.2. Fr.6.2 (21.9 g) was divided into 8 subfractions (Fr.6.2.1–Fr.6.2.8) over silica gel using $CHCl_3$-MeOH (7:1) as a solvent. Fr.6.2.4 was separated by HPLC (CH_3CN/H_2O, 17:83) to give **4** (21 mg) and **5** (17 mg), respectively. Separation of Fr.6.2.6 over a C18 column (MeOH/H_2O, 45:55) yielded 6 subfractions (Fr.6.2.6.1–Fr.6.2.6.6). Fr.6.2.6.2 was separated by HPLC (CH_3CN/H_2O, 1:3) to afford **1** (18 mg). Fr.6.2.7 was divided into 3 subfractions (Fr.6.2.7.1–Fr.6.2.7.3) over a C18 column (MeOH/H_2O, 35:65). Fr.6.2.7.2 was separated by HPLC (CH_3CN/H_2O, 1:3) to give **7** (42 mg).

Fr.7 (7.8 g) was separated using a Sephadex (LH-20) CC eluted with $CHCl_3$-MeOH (1:1) to yield Fr.7.1–Fr.7.4. Fr.7.2 (1.2 g) was separated over a C18 column (MeOH/H_2O, 35:65) to yield 3 subfractions (Fr.7.2.1–Fr.7.2.3). Fr.7.2.3 was further purified by HPLC (CH_3CN/H_2O, 1:2) to give **2** (17 mg) and **3** (3.5 mg), respectively. Fr.7.3 was separated by silica gel CC using $CHCl_3$-MeOH (12:1) to afford 3 subfractions (Fr.7.3.1–Fr.7.3.3). Fr.7.3.1 was separated by HPLC (MeOH/H_2O, 1:4) to give **8** (35 mg).

4.3.1. 2, 5-Dihydroxy-4-methoxy-phenanthrene 2-O-β-D-glucopyranoside (**1**)

Colorless colloidal solid; mp 166–169 °C; $[\alpha]$ $^{25}_D$ −52 (c 0.8, MeOH); UV (MeOH) λ_{max} (log ε) 214.5, 254, 283.5 and 313.5 nm; IR (KBr) ν_{max} 3427, 1614, 1384, 1261, 1073, 819, and 595 cm^{-1}; for ^1H NMR and ^{13}C spectroscopic data NMR, see Table 1; HR-ESI-MS m/z 425.1208 (calcd for $C_{21}H_{22}O_8Na$, 425.1208).

4.3.2. 2,5-Dihydroxy-4-methoxy-phenanthrene 2-O-β-D-apiofuranosyl-(1–6)-β-D-glucopyranoside (**2**)

Yellowish colloidal solid; mp 206–210 °C; $[\alpha]$ $^{25}_D$ −133 (c 0.2, MeOH); UV (MeOH) $_{max}$ (log ε) 215.0, 254, 283.5 and 315.0 nm; IR (KBr) ν_{max} 3434, 1615, 1430, 1261, 1068, 821, and 619 cm^{-1}; for ^1H NMR and ^{13}C NMR spectroscopic data, see Table 1; HR-ESI-MS *m*/*z* 557.1629 (calcd for $C_{26}H_{30}O_{12}Na$, 557.1629).

4.3.3. 2,5-Dihydroxy-4-methoxy-phenanthrene 2-O-α-L-rhamnopyranosyl-(1–6)-β-D-glucopyranoside (**3**)

Yellowish colloidal solid; mp 194–200 °C; $[\alpha]$ $^{25}_D$ −144 (c 0.5, MeOH); UV (MeOH) $_{max}$ (log ε) 214.5, 254, 283.5, and 314.5 nm; IR (KBr) ν_{max} 3441, 1615, 1454, 1268, 1063, 828, and 599 cm^{-1}; for ^1H NMR and ^{13}C NMR spectroscopic data, see Table 1; HR-ESI-MS *m*/*z* 571.1794 (calcd for $C_{27}H_{32}O_{12}Na$, 571.1794).

4.3.4. 5-Methoxy-2,4,7,9S-tetrahydroxy-9,10-dihydrophenanthrene (**4**)

Yellowish powder; mp 157–161 °C; $[\alpha]$ $^{25}_D$ +69 (c 0.1, MeOH); UV (MeOH) $_{max}$ (log ε) 211.0, 274.5, and 307.0 nm; IR (KBr) ν_{max} 3420, 1735, 1622,1455, 1156,1037, 873, and 672 cm^{-1}; for ^1H NMR and ^{13}C NMR spectroscopic data, see Table 2; HR-ESI-MS *m*/*z* 297.0736 (calcd for $C_{15}H_{14}O_5Na$, 297.0736).

4.3.5. 4-Methoxy-2,5,7,9S-tetrahydroxy-9,10-dihydrophenanthrene (**5**)

An isomer of compound 4: yellowish powder; mp 167–172 °C; $[\alpha]$ $^{25}_D$ +62 (c 0.15, MeOH); UV (MeOH) $_{max}$ (log ε) 211.5, 274.5 and 306.0 nm; IR (KBr) ν_{max} 3439, 1636, 1615, 1438, 1161, 871, and 617 cm^{-1}; for ^1H NMR and ^{13}C NMR spectroscopic data, see Table 2; HR-ESI-MS *m*/*z* 297.0736 (calcd for $C_{15}H_{14}O_5Na$, 297.0736).

4.3.6. 5-Methoxy-4,7,9S-trihydroxy-9,10-dihydrophenanthrene (**6**)

Yellowish powder; mp 166–172 °C; $[\alpha]$ $^{25}_D$ +80 (c 1.5, MeOH); UV (MeOH) $_{max}$ (log ε) 212.0, 272.5 and 303.0 nm; IR (KBr) ν_{max} 3434, 1626, 1458, 1384, 1161, and 617 cm^{-1}; for ^1H NMR and ^{13}C NMR spectroscopic data, see Table 1; HR-ESI-MS *m*/*z* 281.0784 (calcd for $C_{15}H_{14}O_4Na$, 281.0784).

4.3.7. 4-Methoxy-2,5,9R-trihydroxy-9,10-dihydrophenanthrene 2-O-β-D-glucopyranoside (**7**)

Yellowish colloidal solid; mp 179–185 °C; $[\alpha]$ $^{25}_D$ −60 (c 0.9, MeOH); UV (MeOH) $_{max}$ (log ε) 211.0, 270.0 and 302.0 nm; IR (KBr) ν_{max} 3398, 1612, 1450, 1302, 1261, 1166, 905, 799, and 625 cm^{-1}; for ^1H NMR and ^{13}C NMR spectroscopic data, see Table 1; HR-ESI-MS *m*/*z* 443.1318 (calcd for $C_{21}H_{24}O_9Na$, 443.1318).

4.3.8. 1,2,5,9R-Tetrahydroxy-9,10-dihydrophenanthrene 5-O-β-D-glucopyranoside (**8**)

Yellowish colloidal solid; mp 164–168 °C; $[\alpha]$ $^{25}_D$ −46 (c 0.3, MeOH); UV (MeOH) λ_{max} (log ε) 211.0, 275.0 and 302.0 nm; IR (KBr) ν_{max} 3420, 1622, 1459, 1384, 1232, 1156, 1073, and 618 cm^{-1}; for ^1H NMR and ^{13}C NMR spectroscopic data, see Table 1; HR-ESI-MS *m*/*z* 443.1156 (calcd for $C_{21}H_{24}O_9Na$, 443.1156).

4.4. Acid hydrolysis of compounds **1**–**3**, **7** and **8**

Compounds **1–3** (1 mg) in dioxane (1 mL) and 10% H_2SO_4 (1 mL) were heated at 95 °C for 3 h. After neutralization with 0.2 M $Ba(OH)_2$, the aglycone was extracted with CH_2Cl_2, with the aqueous residue filtered through absorbent gauze, and the resulting filtrate concentrated under reduced pressure. Each sugar mixture was treated with Ac_2O (0.5 mL) and pyridine (0.25 mL) at 95 °C for 12 h. After cooling, each mixture was poured into ice-water, stirred and stored for several hours. Each residue was then partitioned between H_2O and CH_2Cl_2. The CH_2Cl_2 layer was washed with H_2O (3 × 2.5 mL), with each CH_2Cl_2 soluble was analyzed by GC–MS; compounds were identifier by comparison with derivatives of authentic sugars (Antonov et al., 2009). The absolute configuration of the sugar was determined by the Klyne's rule (Klyne, 1950).

Compounds **7–8** (3 mg) were treated as described for compounds **1–3** to give a sugar. The sugar was confirmed by comparison of its derivative with that of authentic sample on GC–MS and by its optical rotation.

4.5. Cell culture

RAW264.7 cells and HeLa cells were grown in Dulbecco's modified Eagle's medium (DMEM) (Invitrogen, Carlsbad, CA, USA) supplemented with 1% penicillin/streptomycin and 10% fetal calf serum (Gibco-Invitrogen). HepG2 cells were maintained in RPMI 1640 medium (Invitrogen) supplemented with 1% penicillin/streptomycin and 10% fetal calf serum at 37 °C in a humidified atmosphere containing 5% CO_2. For experiments of nitric oxide content, RAW264.7 cells were maintained in medium devoid of Phenol Red (Invitrogen).

4.6. Cell proliferation assay

Cell proliferation was assayed as described previously (Yang et al., 2011). In brief, 1×10^4 RAW264.7 cells, HeLa cells, and HepG2 cells were seeded in 96-well plates, and treated with the compounds for 24 h. After AlamarBlue reagent was added to each well, and fluorescence intensity was measured with excitation at 544 nm and excitation at 590 nm using Thermo Scientific Varioskan Flash Multimode Reader. Cytotoxicity was defined as the ratio of the fluorescence intensity in test wells compared to solvent control wells (0.1% DMSO). The assay was conducted 3 times in triplicate.

4.7. Measurement of nitric oxide content

The RAW264.7 macrophages were seeded in 96-well plates at 1×10^4 cells/well, and pretreated with various concentrations of compounds **1–12** for 2 h, followed by 1 μg/mL LPS for an additional 24 h. After that the cell culture medium was used for NO measurements using a commercial available kit (Beyotime, Haimen, China). Nitrite production was measured at OD_{550}. The assay was conducted 3 times in triplicate. Percentage inhibition was calculated using the following equation:

$$\%\text{Inhibition} = (A - B)/(A - C) \times 100$$

A: LPS (+), sample (−); *B*: LPS (+), sample (+); *C*: LPS (−), sample (−).

4.8. Western blotting

The RAW264.7 macrophages were pretreated with various concentrations (1, 10, 50 μM) of compounds **1** and **4** for 2 h and then stimulated with LPS (1 μg/mL) for 30 min (phospho-p38 and phospho-JNK), 20 min (phospho-IκBα), or 18 h (iNOS). Subsequently the cells were lysed in RIPA buffer (Beyotime, Haimen, China) supplemented with a cocktail of protease and phosphatase inhibitors (Pierce, Rockford, IL, USA). The protein concentrations were determined using a BCA protein assay kit (Pierce). Aliquots of total cell lysates (50 μg) were mixed in loading buffer, boiled for 5 min, and subjected to SDS–PAGE (10%). Following electrophoresis, the proteins were transferred to nitrocellulose membranes, blocked with 5% bovine serum albumin and then incubated at 4 °C overnight with anti-phospho-p38 MAPK, anti-p38 MAPK, anti-GAPDH (Epitomics, Burlingame, CA, USA), anti-iNOS, anti-phospho-JNK, anti-JNK, or anti-phospho-IκBα (Cell Signaling Technology, Danvers, MA, USA) antibodies. Membranes were then incubated with a horseradish peroxidase-conjugated secondary antibody (Santa Cruz Biotechnology, Santa Cruz, CA, USA) for 2 h at room temperature and developed using an enhanced chemiluminescence detection system (Amersham Bioscience, Piscataway, NJ, USA). The intensity of each signal was determined by a computer image analysis system (Quantity One, Bio-Rad, Hercules, CA, USA).

4.9. Statistical analysis

All statistical calculations were carried out using GraphPad Prism 5.01. The results were expressed as the mean ± standard error of mean of 3 independent experiments with individual values. The data were subjected to a one-way analysis of variance (ANOVA); $p < 0.05$ was considered to be statistically significant.

Acknowledgments

This work was supported by National New Drug Innovation Major Project of China (2011ZX09307-002-02), Key Projects in the National Science & Technology Pillar Program (2011BAC09B04), Knowledge Innovation Program of the Chinese Academy of Sciences (No. XBCD-2011-007) and "Twelfth Five-Year" Chinese Herbal Medicines Breeding Research of Sichuan Province.

Appendix A. Supplementary data

Supplementary data associated with this article can be found, in the online version, at http://dx.doi.org/10.1016/j.phytochem.2013.08.008.

References

Adriána, K., Andrea, V., Judit, H., 2008. Natural phenanthrenes and their biological activity. Phytochemistry 69, 1084–1110.

Antonov, A.S., Avilov, S.A., Kalinovsky, A., Anastyuk, S.D., Dmitrenok, P.S., Kalinin, V.I., Taboada, S., Bosh, A., Avila, C., Stonik, V., 2009. Triterpene glycosides from antarctic sea cucumbers. 2. Structure of achlioniceosides A_1, A_2 and A_3 from the sea cucumber *Achlionice wiolaecuspidata* (=*Rhipidothuria racowitzai*). J. Nat. Prod. 72, 33–38.

Badger, A.M., Cook, M.N., Lark, M.W., Newman-Tarr, T.M., Swift, B.A., Nelson, A.H., Barone, F.C., Kumar, S., 1998. SB 203580 inhibits p38 mitogen-activated protein kinase, nitric oxide production, and inducible nitric oxide synthase in bovine cartilage-derived chondrocytes. J. Immunol. 161, 467–473.

Bennett, B.L., Sasaki, D.T., Murray, B.W., Sakata, S.T., Xu, W., Leisten, J.C., Motiwala, A., Pierce, S., Satoh, Y., Bhagwat, S.S., Manning, A.M., Anderson, D.W., 2001. SP600125, an anthrapyrazolone inhibitor of Jun N-terminal kinase. Proc. Natl. Acad. Sci. USA 98, 13681–13686.

Chen, C.C., Wang, J.K., Lin, S.B., 1998. Antisense oligonucleotides targeting protein kinase C-α, -βI, or -δ but not -η inhibit lipopolysaccharide-induced nitric oxide synthase expression in RAW 264.7 macrophages: involvement of a nuclear factor κB-dependent mechanism. J. Immunol. 161, 6206–6214.

Datla, P., Kalluri, M.D., Basha, K., Bellary, A., Kshirsagar, R., Kanekar, Y., Upadhyay, S., Singh, S., Rajagopal, V., 2010. 9,10-Dihydro-2,5-dimethoxyphenanthrene-1,7-diol, from *Eulophia ochreata*, inhibits inflammatory signalling mediated by Toll-like receptors. Br. J. Pharmacol. 160, 1158–1170.

Devkota, H.P., Watanabe, M., Watanabe, T., Yahara, S., 2012. Diplomorphanins A and B: new C-methyl flavonoids from *Diplomorpha canescens*. Chem. Pharm. Bull. 60, 554–556.

Fan, C., Wang, W., Wang, Y., Qin, G., Zhao, W., 2001. Chemical constituents from *Dendrobium densiflorum*. Phytochemistry 57, 1255–1258.
Guzik, T.J., Korbut, R., Adamek-Guzik, T., 2003. Nitric oxide and superoxide in inflammation and immune regulation. J. Physiol. Pharmacol. 54, 469–487.
Ito, M., Matsuzaki, K., Wang, J., Daikonya, A., Wang, N., Yao, X., Kitanaka, S., 2010. New phenanthrenes and stilbenes from *Dendrobium loddigesii*. Chem. Pharm. Bull. 58, 628–633.
Karin, M., 1995. The regulation of AP-1 activity by mitogen-activated protein kinases. J. Biol. Chem. 270, 16483–16486.
Khan, S., Shin, E.M., Choi, R.J., Jung, Y.H., Kim, J., Tosun, A., Kim, Y.S., 2011. Suppression of LPS-induced inflammatory and NF-κB responses by anomalin in RAW 264.7 macrophages. J. Cell. Biochem. 112, 2179–2188.
Khurelbat, D., Densmaa, D., Sanjjav, T., Gotov, C., Kitamura, C., Shibuya, H., Ohashi, K., 2010. Artemisioside, a new monoterpene glucoside from the aerial parts of *Artemisia ordosica* (*Asteraceae*). J. Nat. Med. 64, 203–205.
Klyne, W., 1950. The configuration of the anomeric carbon atomsinsome cardiac glycosides. Biochem. J. 47, Xii–Xiii.
Korhonen, R., Lahti, A., Kankaanranta, H., Moilanen, E., 2005. Nitric oxide production and signaling in inflammation. Curr. Drug Targets 4, 471–479.
Lee, J.C., Laydon, J.T., McDonnell, P.C., Gallagher, T.F., Kumar, S., Green, D., McNulty, D., Blumenthal, M.J., Heys, R.J., Landvatter, S.W., Strickler, J.E., McLaughlin, M.M., Siemens, I.R., Fisher, S.M., Livi, G.P., White, J.R., Adams, J.L., Young, P.R., 1994. A protein kinase involved in the regulation of inflammatory cytokine biosynthesis. Nature 372, 739–746.
Lee, Y.H., Park, J.D., Baek, N.I., Kim, S.I., Ahn, B.Z., 1995. In vitro and in vivo antitumoral phenanthrenes from the aerial parts of *Dendrobium nobile*. Planta Med. 61, 178–180.
Lee, C.L., Chang, F.R., Yen, M.H., Yu, D., Liu, Y.N., Bastow, K.F., Susan, L., Morris, N., Wu, Y.C., Lee, K.H., 2009. Cytotoxic phenanthrenequinones and 9,10-dihydrophenanthrenes from *Calanthe arisanensis*. J. Nat. Prod. 72, 210–213.
Li, Y., Wang, C.L., Wang, Y.J., Guo, S.X., Yang, J.S., Chen, X.M., Xiao, P.G., 2009. Three new bibenzyl derivatives from *Dendrobium candidum*. Chem. Pharm. Bull. 57, 218–219.
Lin, T.H., Chang, S.J., Chen, C.C., Wang, J.P., Tsao, L.T., 2001. Two phenanthraquinones from *Dendrobium moniliforme*. J. Nat. Prod. 64, 1084–1086.
Liu, Y., Jiang, J.H., Zhang, Y., Chen, Y.G., 2009. Chemical constituents of *Dendrobium aurantiacum var. denneanum*. Chem. Nat. Compd. 45, 525–527.
Mendes, S.D.S., Candi, A., Vansteenbrugge, M., Pignon, M.R., Bult, H., Boudjeltia, K.Z., Munaut, C., Raes, M., 2009. Microarray analyses of the effects of NF-kappaB or PI3K pathway inhibitors on the LPS-induced gene expression profile in RAW264.7 cells: synergistic effects of rapamycin on LPS-induced MMP9-overexpression. Cell. Signalling 21, 1109–1122.
Okamura, N., Nohara, T., Yagi, A., Nishioka, I., 1981. Studies on the constituents of *Zizyphi fructus*. III. Structures of dammarane-type saponins. Chem. Pharm. Bull. 29, 676–683.
Ono, K., Han, J., 2000. The p38 signal transduction pathway activation and function. Cell. Signalling 12, 1–13.
Quivy, V., Lint, C.V., 2004. Regulation at multiple levels of NF-κB-mediated transactivation by protein acetylation. Biochem. Pharmacol. 68, 1221–1229.
Resnick, S.M., Gibson, D.T., 1996. Regio- and stereospecific oxidation of fluorene, dibenzofuran, and dibenzothiophene by naphthalene dioxygenase from *Pseudomonas* sp. strain NCIB 9816-4. Appl. Environ. Microbiol. 62, 4073–4080.
Shu, Y., Guo, S.X., Chen, X.M., Wang, C.L., Yang, J.S., 2004. On the chemical constituents of *Dendrobium nobil*. Chin. Pharm. J. 6, 421–422.
Sung, M.J., Davaatseren, M., Kim, W., Park, S.K., Kim, S., Hur, H.J., Kim, M.S., Kim, Y., Kwon, D.Y., 2009. Vitisin A suppresses LPS-induced NO production by inhibiting ERK, p38, and NF-kappaB activation in RAW 264.7 cells. Int. Immunopharmacol. 9, 319–323.
Takayanagi, T., Ishikawa, T., Kitajima, J., 2003. Sesquiterpene lactone glucosides and alkyl glycosides from the fruit of cumin. Phytochemistry 63, 479–484.
Thirunavukkarasu, C., Watkins, S.C., Gandhi, C.R., 2006. Mechanisms of endotoxin induced NO, IL-6, and TNF-α production in activated rat hepatic stellate cells: role of p38 MAPK. Hepatology 44, 389–398.
Wang, H.K., Zhao, T.F., 1985. Dendrobine and 3-hydroxy-2-oxodendrobine from *Dendrobium nobile*. J. Nat. Prod. 48, 796–801.
Wang, X.Y., Ke, C.Q., Tang, C.P., Yuan, D., Ye, Y., 2009. 9,10-Dihydrophenanthrenes and -henanthrenes from *Juncus setchuensis*. J. Nat. Prod. 72, 1209–1212.
Yang, L., Qin, L.H., Annie Bligh, S.W., Bashall, A., Zhang, C.F., Zhang, M., Wang, Z.T., Xu, L.S., 2006a. A new phenanthrene with a spirolactone from *Dendrobium chrysanthum* and its anti-inflammatory activities. Bioorg. Med. Chem. 14, 3496–3510.
Yang, L., Wang, Z., Xu, L., 2006b. Phenols and a triterpene from *Dendrobium aurantiacum var. denneanum* (Orchidaceae). Biochem. Syst. Ecol. 34, 658–660.
Yang, H., Sung, S.H., Kim, Y.C., 2007a. Antifibrotic phenanthrenes of *Dendrobium nobile* stems. J. Nat. Prod. 70, 1925–1929.
Yang, L., Wang, Y., Zhang, G., Zhang, F., Zhang, Z., Wang, Z., Xu, L., 2007b. Simultaneous quantitative and qualitative analysis of bioactive phenols in *Dendrobium aurantiacum var. denneanum* by high-performance liquid chromatography coupled with mass spectrometry and diode array detection. Biomed. Chromatogr. 21, 687–694.
Yang, L.J., Chen, Q.F., Wang, F., Zhang, G.L., 2011. Antiosteoporotic compounds from seeds of *Cuscuta chinensis*. J. Ethnopharmacol. 135, 553–560.
Yoshikawa, K., Ito, T., Iseki, K., Baba, C., Imagawa, H., Yagi, Y., Morita, H., Asakawa, Y., Kawano, S., Hashimoto, T., 2012. Phenanthrene derivatives from *Cymbidium* great flower marie laurencin and their biological activities. J. Nat. Prod. 75, 605–609.
Zhang, G.N., Bi, Z.M., Wang, Z.T., Xu, L.S., Xu, G.J., 2003. Advances in studies on chemical constitutents from plants of *Dendrobium* Sw. Chin. Tradit. Herbal Drugs 34, S5–S8.
Zhang, G.N., Zhong, L.Y., Bligh, S.W.A., Guo, Y.L., Zhang, C.F., Zhang, M., Wang, Z.T., Xu, L.S., 2005. Bi-bicyclic and bi-tricyclic compounds from *Dendrobium thyrsiflorum*. Phytochemistry 66, 1113–1120.
Zhang, X., Xu, J.K., Wang, J., Wang, N.L., Hiroshi, K., Sumumu, K., Yao, X.S., 2007. Bioactive bibenzyl derivatives and fluorenones from *Dendrobium nobile*. J. Nat. Prod. 70, 24–28.
Zhang, X., Tu, F.J., Yu, H.Y., Wang, N.L., Wang, Z., Yao, X.S., 2008. Copacamphane, picrotoxane and cyclocopacamphane sesquiterpenes from *Dendrobium nobile*. Chem. Pharm. Bull. 56, 854–857.
Zhao, W., Ye, Q., Tan, X., Jiang, H., Li, X., Chen, K., Kinghorn, A.D., 2001. Three new sesquiterpene glycosides from *Dendrobium nobile* with immunomodulatory activity. J. Nat. Prod. 64, 1196–1200.